## Физический
## ИНСТИТУТ
### *имени*
### *П.Н.Лебедева*

**Ф  И  А  Н**

L. A. BORISENKO, G. V. SKLIZKOV, O. N. ROSMEJ

# SOLID LOW-DENSITY TARGET STRUCTURE INFLUENCE ON HEAVY ION STOPPING IN PLASMA

# Solid low-density target structure influence on heavy ion stopping in plasma

**L.A. Borisenko[1,2], G.V. Sklizkov[1], O.N. Rosmej[3,4]**

*[1]P.N. Lebedev Physical Institute of the Russian Academy of Sciences, Moscow, Russia*
*[2]Lomonosov Moscow State University, Moscow, Russia*
*[3]GSI Helmholtzzentrum für Schwerionenforschung, Darmstadt, Germany*
*[4]University of Frankfurt, Frankfurt-am-Main, Germany*

## Abstract

Heavy ion stopping effects in plasmas have already been studied for decades. In this article we discuss the specific features of low-density plastic aerogels (cellulose triacetate, CTA). Due to structural effects the energy losses of fast non-relativistic heavy ions in plastic aerogels cannot be described by already existing stopping theories. What additional characteristics should we take into account for this type of solids? Here we discuss the possible mechanisms of low-density structure influence on plasma features for ion stopping.

## 1. <u>Introduction</u>

In early high-power irradiation experiments on low-density targets the structure was reported to have slight or no influence on the major results. Further the distinct unpredicted effects appeared to be connected with initial solid structure, especially when the diagnostic means achieved high resolution and accuracy.

Polymer plastic aerogels, unlike many other low-density materials (foam, dust, nano-snow) have a net-like structure, consisting of macromolecular fibers and globules. That means they are highly regular as regards their spatial structure, so high repeatability was demonstrated in interaction experiments with polymer plastic aerogel targets. However we yet have definite molecular structure in the polymer before irradiation.

Which structural or non-structural effects should we take into account in plasma and which can be neglected? Below we consider the initial phase of soft x-rays irradiation.

Numerous calculations and experiments on stopping power in plasma have been carried out within last decades [1, 2]. Different research conditions, plasma composition and properties were used to obtain quite a strict stopping power dependence on ion energies in different plasma temperatures. Yet classical plasmas obtained from either solid foils or gases and clusters do not cover the whole field.

Low-density plastic aerogels, like cellulose triacetate (CTA) [3, 4] or divinyl benzene [5], have already shown numerous transient effects in terms of laser-plasma interaction experiments. Brillouin and Raman scattering, plasma partial transparency were observed in different scientific centers and discussed earlier. Stochastic structure and significantly subcritical electron densities of extreme low-density plastic aerogels provide perfect conditions for plasma analysis.

The low-density structures [6, 7] were proposed to be used as an additional cover-layer for ICF to raise energy absorption or x-ray conversion efficiency in the hohlraum. In this terms energetic particle stopping in such laser-irradiated targets would become extremely interesting. However heavy ion stopping in low-density solid structures and plasmas obtained from them was not yet studied properly.
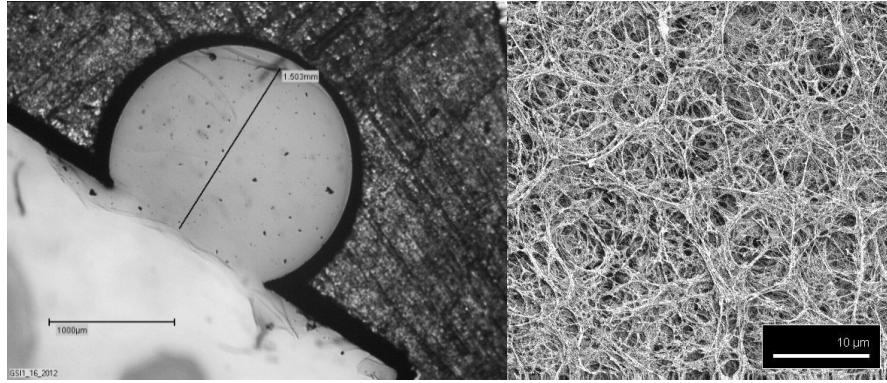
***Fig. 1 Cellulose triacetate (CTA) plastic aerogel: optical image and SEM inner structure***

Atomic physics approach for ion stopping by bound and free electrons in $T_e \sim 1 \div 3 \ [eV]$ plasmas was discussed in [1, 2, 13]. In both cases, for free electrons and Bohr-Bethe-Bloch and Barkas approximations for bound electrons, energy losses are proportional to electron concentration if the projectile velocity is constant. The electron energy or temperature brings an inverse ratio with projectile velocity fixed. The difference in the projectile energies does not make any sense since we speak about fixed non-relativistic velocities. However the projectile energy should be significantly higher than the ionization barrier for the outer shell electrons.

This approach is successfully used for monoatomic classical plasmas or solid films. However, for diatomic plasmas the dependence shape is the same. The CTA plastic aerogels consist of light elements: hydrogen, carbon and oxygen which are close by the atomic mass and thus electron shell structure. Therefore for ion stopping estimations it can be considered nearly diatomic. But do only the same forces resulting in the same function take action in plastic aerogels?

## 2. **Experimental scheme and the target**

Indirect combination experiments were carried out in GSI in 2011-2012 [8, 9, 10. 11]. PHELIX laser and UNILAC heavy ion beam were used simultaneously and with one target (Fig. 2).

The incoming energy from the PHELIX laser system was converted into x-ray spectrum by *Au* pre-target – hohlraum. Thus the 2-3 mg/cc cellulose triacetate (CTA) plastic aerogel was irradiated with broad *Au* x-ray spectrum from the bottom of the hohlraum (Fig. 3). The CTA target was continuously probed with UNILAC heavy ion beam. Time-of-flight (TOF) measurements with diamond stopping detector provided the data on the stopping power before, during and after the laser shot. Time steps of

TOF measurements were determined by heavy ion beam bunch structure and the delay between the laser and the following bunch.
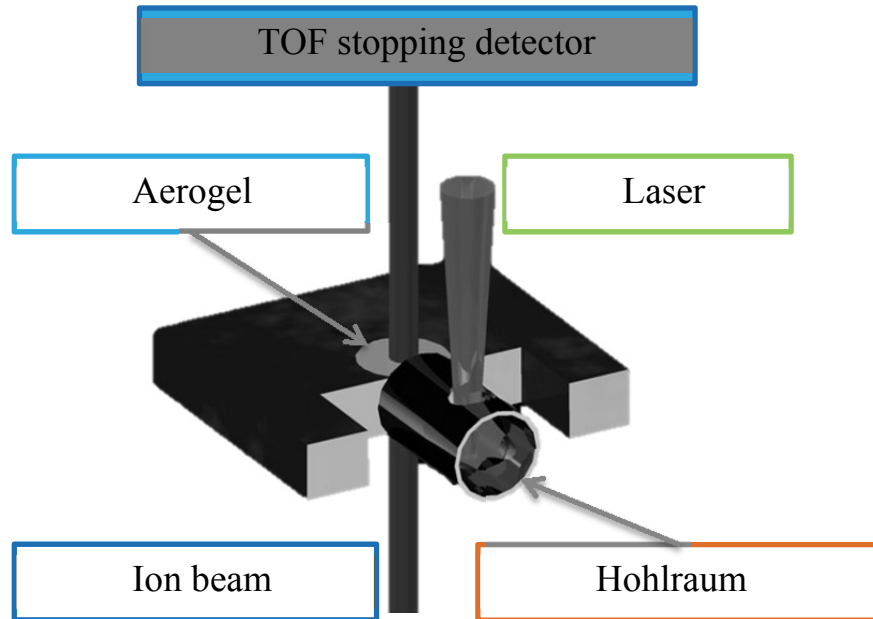


*Fig. 2 Experimental scheme*

Laser pulse parameters were ~150 J within 1.4 ns in the $2\omega$ frequency of Nd. UNILAC ion beam parameters: $Ti^{12+}$ with 4.8 MeV/a.m.u. with total pulse duration of 30 mks. The bunch period was 27.7 ns and bunch duration 3-4 ns.
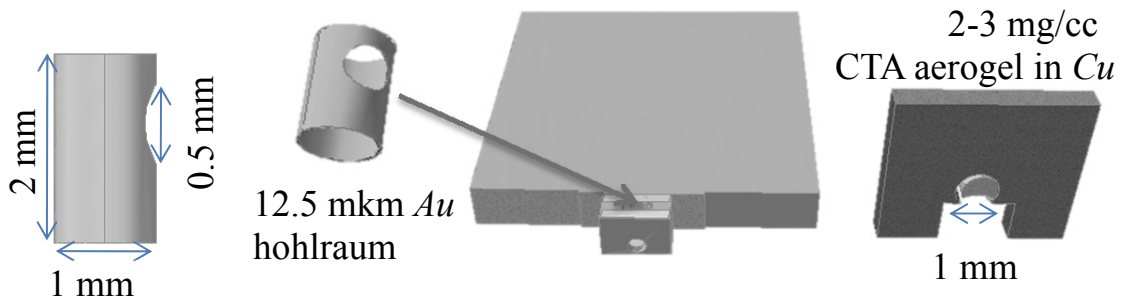


*Fig. 3 Target construction and parameters*

### 3. <u>Transient process effect for heavy ion stopping in CTA plastic aerogels</u>

Indirect irradiation of plastic aerogels by PHELIX laser beam converted into soft x-rays provides milder conditions for target polymer transition into plasma than in direct laser-target interaction. On early times of plastic aerogel irradiation with x-rays from the hohlraum, a decrease of ion stopping power was observed in the target. Char-

acteristic time for the observed process was 3-4 ns. Further increase of ion stopping power was expected due to ion scattering on plasma hot free electrons.

As the stopping power was observed by TOF measurements we present the data in time units [8]. The time on the axes represents the position of the ion bunch center oberved in comparison to the expected one. Measurements of the delay between the ion bunch in cold CTA target and in vacuum were measured and determine the vacuum levels for dynamical plasma stopping. The average delay varies for the two CTA plastic aerogel densities used and is 2.2 ns higher for the 3mg/cc samples than for 2 mg/cc. Ion stopping power in x-ray heated polymer aerogel is time-dependent.

The delay between the beginning of the laser pulse and the middle of the closest ion bunch was used as a trigger. The delay of each bunch in each target was compared to the one in vacuum. The zero level for X-axes is marked by the laser beam arrival on the hohlraum while for Y-axes it is attached to the level of the bunch stopping in the cold target (see Fig. 4).

The below-zero data points are yet significantly higher than the vacuum level for 2 mg/cc and 3 mg/cc target densities. This decrease of the stopping power is visible within 4 ns from the laser beam front arrival which is significantly longer than the pulse duration.

What would we have expected [12, 13, 14]? For the two states of matter, solid plastic aerogel and ionized gas of finite temperature, the energy losses can be written in the same form:

$$\left(-\frac{dE}{dx}\right) = F_1(Z^2, V, n_e)\left(ln\big(f_1(V)\big) - f_2(V)\right) + F_2(Z^3, v_e, n_e, V),$$

(1)

$$where \; F_1(Z^2, V, n_e) = \frac{const \cdot Z^2 e^4 n_e}{V^2 m_e} \; .$$

$Z$ is the projectile charge and $V$ – projectile velocity. The majority of the stopping effect [1, 2, 12] in the Coulomb single-track interaction approximation is caused by the first term of the equation (1) and particularly by the $F_1$ function. The rest can only scale the energy losses and cause no significant changes in the functional behavior. In case of UNILAC Ti ion beam the projectile velocity is constant; therefore we shall examine the $F_1(Z^2, V, n_e)$ function. Heating of solid plastic aerogel alters electron concentration and electron energy distribution, thus electron velocity $v_e$ and temperature.

During the transient process from solid plastic aerogel to homogeneous plasma the concentration of free electrons rises significantly – up to $n_e \sim 10^{20} \div 10^{22}$. The

6

upgrowth of the concentration on the early times of irradiation can be approximated linear as the radiation intensity is constant. This leads to nearly linear growth of the energy losses, $-dE/dx$. Further exponential decline is due to hydrodynamic expansion of the plasma from the region of interest and thus exponential decline of the concentration. Electron temperature or, in case of bound electrons, ionization potential or energy do not make any influence on the energy losses as during the whole process it is significantly lower than the projectile energy.

However none of the stated arguments point out the reasons for the ion stopping power fall on the early interaction times. Next we discuss the possible explanations for the effect.

### 4. <u>The target structural quasistability</u>

Immediate dissolution of the target structure and ionization seems to be a good approach for powerful lasers. However for strict discussion of the effects we shall consider this time finite. In our case slow x-ray heating process provided time resolution suitable to discuss transient processes in structure.

The CTA low-density plastic aerogel was irradiated with soft x-rays from $Au$ hohlraum (Fig. 3).

We consider the incoming energy from the PHELIX laser system being converted into Planckian-like spectrum with $T_{pl}$=45 eV [5]. The laser pulse parameters of ~150 J within ~1ns mean up to 120 J of the blackbody internal energy.

The size of the laser spot on the hohlraum wall is 200 mkm. This equals radiation intensity $I_{laser} = 10^{13}\ W/cm^2$. Initial heating of the hohlraum with PHELIX laser beam forms the ~10 eV blackbody. The temperature is determined by incoming and outgoing energy fluxes:

$$(2)\ I_{laser} \cdot s = W_{laser} = \sigma T^4(S + s) + W_{abs} + W_{sc} \approx \sigma T^4(S + s)\,,$$

Where $s$ is area of the focal hole of the hohlraum and $S$ is the area of the radiation hole in the plastic aerogel direction. We neglect high (~800 eV) temperature and low intensity scattered radiation and consider all the absorbed energy being reradiated. However the effective temperature for plastic aerogel heating from the hohlraum was published to be $T_{pl}$=45 eV, so the energy density is recalculated from the Plank integral:

$$(3)\ u(\omega, T) = \frac{1}{\pi^2 c^3} \frac{\hbar\omega^3}{\exp\left(\hbar\omega/kT\right) - 1}\,,$$

$$(4)\ w(T) = \int_0^\infty u\,(\omega, T)d\omega = \frac{\pi^2(kT)^4}{(\hbar c)^3} \approx 5.3 \cdot 10^{21}\ eV\!\big/\!_{cm^3}\ .$$

A blackbody with fixed internal energy will cool, irradiating by Stefan-Boltzmann law. So the effective lifetime of the source – radiation decrease by a factor of $e$ – may be estimated by:

$$(5)\ W = W_0 \cdot \exp\left(-\frac{ct}{4L}\right)\ .$$

Here $W_0$ is 120 J – total blackbody energy, $t$ – time, $L$ – characteristic length. Now we estimate the blackbody cooling time (down to 1/e of initial energy) as: $t_{cool} \approx 5 \cdot 10^{-9}s$. This is less but compatible by the order of magnitude with x-ray diode data.

Strong back scattering of the laser beam energy to the focal 0.8 mm hole of the hohlraum (Fig. 1) and extremely energetic (up to 800 eV) γ-photons emitted into the foam during the laser pulse duration are negligible for CTA ionization process. Weak Planckian-like radiation onto the plastic aerogel compensates neglected energy losses from the hohlraum. Hence we consider the simplification of no losses from the hohlraum and Planckian x-ray spectrum. Energy flux comes only from the bottom of the cylinder, directly onto the polymer. Within early times of x-ray – polymer interaction we can consider blackbody (hohlraum) spectra stable and temperature and irradiated energy constant because of relatively slow thermal changes. The maximum Plankian energy absorbed by the polymer is:

$$(6)\ E_{Pl} = \frac{c}{4}w \cdot s \cdot t \approx 10^{20}t\ [eV],\ \ t\ \text{in}\ [ns]\ .$$

Using CTA polymer plastic aerogels of 2-3 mg/cc density results in to subcritical electron densities in plasma. In this case we may consider the substance transparent throughout the interaction process. CTA chemical formulae is $[C_6H_7O_2\ (OCOCH_3)_3]_n$, with average element mass of 8 a.u. Each monomer has 38 molecular bonds and is asymmetrical with a hexagon base. Average bond strength in such polymer is 130-200 kcal/mol which means 5-8 eV per atom. Now we can recalculate density (2 mg/cc) of the initial target into bonds "concentration" and primary estimate energy and time for molecular structure dissolution:

$$(7)\ n_{bond} = \frac{N_{bond}}{V} = \frac{\rho}{m_{av}} \approx 1.3 \cdot 10^{20}\left[\frac{1}{cc}\right]\ ,$$

$$(8)\ E \sim n_{bond} \cdot \varepsilon_{av} \cdot V \approx 2 \cdot 10^{19}[eV]\ .$$

Comparing $E$ from (7) with source energy $E_{Pl}$ from (4) we get:

$$(9) \ t \approx 5 \cdot 10^{-1}[ns] -$$

lower-bond time interval for molecules dissolution in the 2 mg/cc CTA plastic aerogel target. This time is counted from the laser beam backfront.

As a result we may have visible ion stopping decrease within first nanoseconds after laser beam arrival on the hohlraum due to the target structure. This effect may be explained by different ion-scattering mechanisms in plasma and in solid structures.

Initial plastic aerogel $[C_6H_7O_2 (OCOCH_3)_3]_n$ is a stable and complicated 3D network. Its structure is formed by molecular, Van der Waals and hydrogen bonds. So as the target temperature rises, significant part of high-order interactions with the whole structure is replaced with single-track ion scattering on plasma hot free electrons. Dipole and polarization interactions, which are neglected in classical scattering theories, decrease with structure mobility increase.

On the other hand, partially dissolved CTA plastic aerogel forms a quasi-lattice. So the effect similar to solid state channeling may be observed due to significantly different electron and ion temperatures on the early times of aerogel heating. That means while the unbound electrons form

Partially dissolved and ionized CTA tends to minimize the energy losses, forming a channel. The Lindhard angle defines the transitional structure of the material. To ease the calculations we may estimate potential of the molecular or atomic remnants by Coulomb potential:

$$(10) \quad \frac{mV^2}{2} = \frac{m(V_0 sin\theta)^2}{2} \rightarrow E = E_0 sin^2\theta; \ V = V_0 sin\theta,$$

$$U = \frac{Z_1 Z_2 e^2}{d/2} \rightarrow \frac{Z_1 Z_2 e^2}{d/2} = E_0 sin^2\theta,$$

$$(11) \quad sin\theta = \sqrt{\frac{2Z_1 Z_2 e^2}{E_0 d}} \approx \theta.$$

Here we operate with initial ion energy $E_0$ and quasi-period of CTA plastic aerogel structure $d$. The estimation (11) is valid for single-component lattice but can yet be used in our case, if we use the average charge between carbon and oxygen to define the quasi-lattice. We do not take into account light and thus spatially unstable hydrogen ions.

## 5. Recombination possibility

One of the possible mechanisms for the stopping power reduction is recombination of the plasma free electrons with $Ti^{20+}$ ions. Reactions to be considered are: three-body recombination, photo recombination, dielectronic recombination and dissociative recombination for the earliest times of x-ray heating. The cross-sections differ and should be carefully checked for each case. However, the simplest way to check the probability of all the processes is to compare ion and electron directed velocities. To drive recombination, velocities should be of the same order.

On the early times of plastic aerogel heating by soft x-rays electron temperature of $T_e \sim 1 \div 2\ eV$ is observed [6]. $Ti$ energies are 4.77÷4.8 MeV/m.a.u. which means 230 MeV per ion.

Each ion influences surrounding electrons by the Coulomb force:

$$(12)\ F_{ie} = \frac{Z_{eff}e^2}{r^2}.$$

Since we are interested in maximum gain in energy and directed velocity for the electron, we shall consider the nearest one to $Ti$ ion. Thus the non-screened effective ion charge is $Z_{eff} = Z \approx 12$ throughout the interaction time.

Plasma screening limits the Coulomb force influence by two Debye radii. As the energy and the velocity of the $Ti$ ion change negligibly if not scattered, the time of interaction with a single electron is defined by ion's time-of-flight:

$$(13)\ t_i = \frac{2r_D}{V_i} \approx \frac{r_D}{V_i}\ for\ acceleration, \qquad where\ r_D = \sqrt{\frac{T_e}{4\pi n_e e^2}} \approx 10^{-7}[cm].$$

The average distance between the unbound electrons in plasma is $\sim n_e^{-1/3}$. This determines the average initial electron-$Ti$ ion distance for acceleration. On the initial times of x-ray interaction with the plastic aerogel target, plasma free electron concentration $n_e$ is of the same order with $n_{bond}$ from (7). Here we consider the part of electron distribution function with initial velocities equal zero or co-directed with the ion beam. So the average force on the electron is defined by:

$$(14)\ \overline{F_{ie}} \approx \int_{n^{-\frac{1}{3}}}^{r_D} Q(r)F_{ie}(r)dr\ , \qquad where\ Q(r) = \sqrt[3]{n_e}.$$

We consider the electron being accelerated in the direction of the $Ti$ ion beam flight only. That means the integral is one-dimensional. To check the recombination possibility we compare the final velocity of the accelerated electron $V_e$ with $V_i$:

10

$$(15) \quad \frac{V_e}{V_i} \approx 10^{-2} \ll 1, \quad where \; V_i = \sqrt{\frac{2T_i}{M_i}}, \quad V_e = \frac{t_i \overline{F_{\iota e}}}{m_e}, -$$

that means recombination processes with the ion beam should not be included into the model in our case. However, they may become significant for higher electron temperatures.

### 6. High-order interactions and density fluctuations in plastic aerogels

As we discussed in paragraph 4, the inner structure of the CTA targets remains stable for at least 0.5-1.7 ns from the laser front. Plastic aerogel 3D structure is formed by long molecular fibers. While dissolved, they change to molecular rings and then to atomic ions.

In case of stable and complicated molecular structure we should not neglect high-order interactions. If Coulomb scattering is proportional to $\sim 1/r$, than dipole is $\sim 1/r^2$, quadruple is $\sim 1/r^3$, polarization is $\sim 1/r^4$. That means we do have extra terms in $-dE/dx$ equation (1). The function defining high-order interactions is unknown. However, it will start from a constant classifying the solid structure and will gradually go down together with structure dissolution. On the early times of heating electron concentration does not change significantly, so we observe diminishing of the total stopping power. That means the total energy losses [15, 16, 17] of the ions for any time point consist of two terms:

$$(16) \quad -\frac{dE}{dx}(t) = f_{dipole}(t) + f_{Coulomb}(t).$$

Here $f_{Coulomb}(t)$ is defined by (1) if $V = const, \; n_e = n_e(t)$ and represents Coulomb ionization losses on bound or free electrons, while $f_{dipole}(t)$ introduces high-order interactions with the plastic aerogel structure. As we do not know the strict function for the double-process approximation, we write the terms of equation (16) in the following form:

$$(17) \quad f_{dipole}(t) = -A \cdot \mathrm{erf}(Bt + 2) - A, \quad A, B > 0$$

$$(18) \quad f_{Coulomb}(t) = C \cdot [\mathrm{erf}(Dt - G) + 1]\left(x - \frac{G-2}{D}\right) \cdot \exp\left\{-F\left(x - \frac{G-2}{D}\right)\right\},$$

$$C, D, F, G > 0.$$

We choose smoothed and continuous approximation functions for both, Coulomb and high-order interactions. Minimized parameters $A, B, C, D, F, G$ scale mathematical functions to fit physical processes. Error function

$$(19) \quad \text{erf}(t) = \frac{2}{\sqrt{\pi}} \int_0^t e^{-x^2} dx$$

have been chosen to smooth the Heaviside function which characterizes immediate switching of the process while the strict mechanism is unknown. For $f_{dipole}(t)$ the error function starts together with the laser front arrival on the target. Thus $A$ from (17) defines the energy loss scale for high order-interactions or any other processes involved in stopping power fall on the early times of interaction. $B$ defines the time-scale and accordingly the duration of dissolution process $t \approx 4/B$.

For Coulomb interaction the error function was used with fixed to 1 y-scaling parameter to lessen the number of minimized parameters as it has no physical importance. We used the approximation of linear growth of energy losses and exponential decline, following the electron concentration. Fitting experimental data points with (16) gives the dashed line on Fig.4.

High-order interactions are not a single possible reason for stopping power reduction. We already mentioned channeling effects in paragraph 4 and moreover we should discuss the specifications of experimentally measured parameters for heavy-ion stopping.

The TOF measurements do not give the information on a strict differential value $-dE/dx$, but on integral over the target's thickness $(-dE/dx \cdot \Delta x)$. If we remark inner macrostructure of CTA plastic aerogel from Fig.1, the target density is not a continuous function. It is averaged over volume for solid polymer density inside the fibers and vacuum around them.

That means while the fibers are dissolved the effective polymer density decreases together with electron density $n_e$. Therefore changes the measured stopping power:

$$-\left(\frac{dE}{dx}\right)_{cold} \cdot \Delta x_{cold} \rightarrow -\left(\frac{dE}{dx}\right)_{plasma} \cdot \Delta x_{plasma},$$

(20)

$$\Delta x_{cold} = \sum_{all\ fibers} d_i, \qquad \Delta x_{plasma} = d_{target} \Rightarrow \Delta x_{cold} \ll \Delta x_{plasma}.$$

We can estimate time needed to equalize the ion density and thus $n_e$ over volume of the CTA target if we consider the ion temperature in plasma equal to electron temperature $T = T_e \sim 1 \div 2\ eV$. With the average ion mass $m_{av} = 8\ a.u.$ the ion sonic velocity is estimated:

12

$$（21） \quad v_i = c \sqrt{\frac{kT}{mc^2}} \sim 3 \cdot 10^5 \; cm/s \;\; \Rightarrow$$

$$\tau \sim 10^{-10}$$

That means, the time $\tau$ for target density equalization is significantly low and this process is instantaneous in terms of nanoseconds. So as soon as the absorbed energy is enough for structure dissolution and the ion temperature rises, the electron density falls. This should be considered as an alternative mechanism for the heavy ion energy loss reduction and included into (16) as additional term of the stopping function.
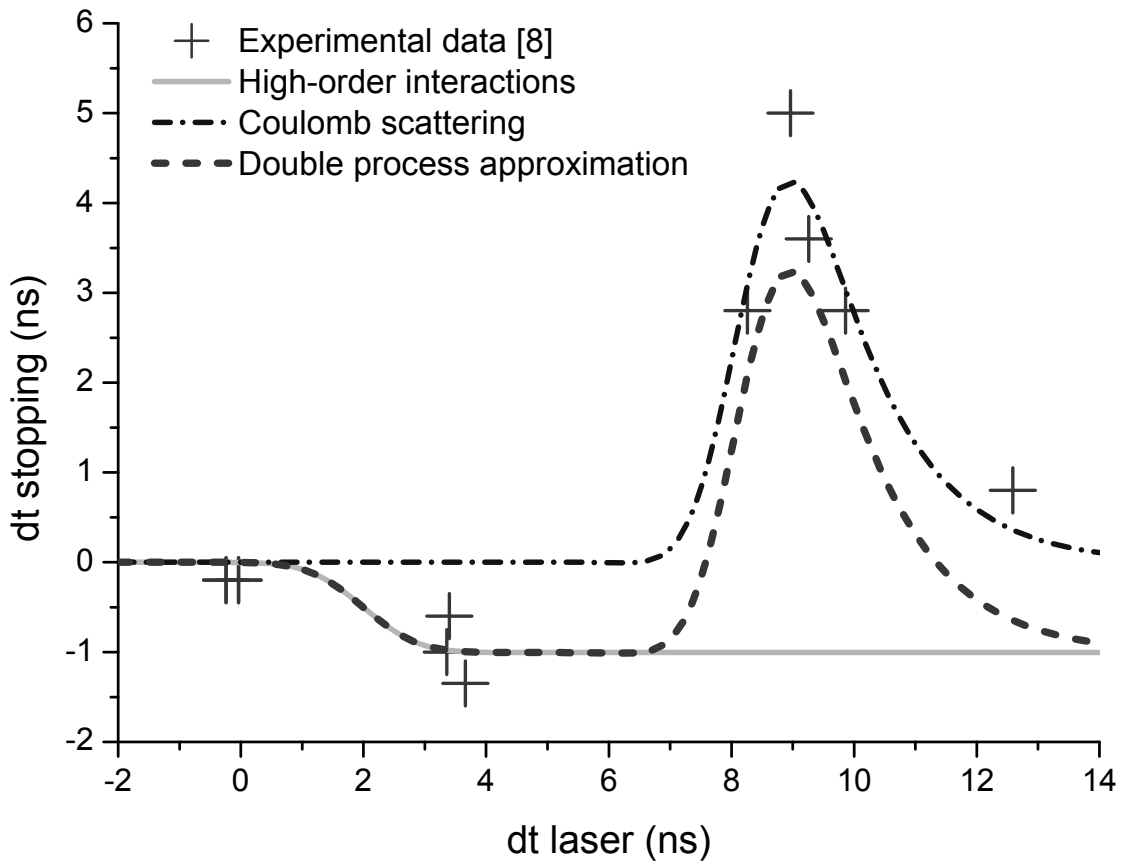


***Fig. 4 Double-process approximation for the stopping power on time dependence.***

## 7. <u>Conclusions</u>

Classical approaches for heavy ion stopping in plasma give correct results for fully ionized CTA plasma, but do not cover the transient process from solid structured material to plasma. However additional processes should be taken in consideration to describe the full-time dynamics of low-density plastic aerogel structure.

Structural effects in low-density CTA targets result in heavy ion energy loss reduction and then restoration to the expected growth. This is explained by four different processes:

a) Reduction and then disappearance of high-order interactions due to long molecular fibers dissolution. On this stage ionization mainly covers molecular bond dissolution and provides structure transition from long fibers to tiny molecular rings and then to atoms or atomic ions. Electron concentration is stable in this phase and has its maximum near the former fibers.

b) Channeling-like effects in quasi lattice of partially dissolved structure. On this stage the electrons are already free to move over the target volume like in metals. At the same time recently ionized carbon and oxygen ions of the target still keep their position thus forming the quasi periodic lattice.

c) Difference in fiber density and average density of the initial CTA target resulting in electron density decrease after the structure's dissolution. On the phase of density equalization the ion density function expands together with electron density to cover uniformly the volume of the CTA target. This results in effective electron density decrease, while the effective volume for heavy ion-target interaction increases.

d) Electron concentration rises significantly due to ionization process and plasma temperature increase. This forms Bethe-like function for heavy ion energy losses in plasma.

That means the transient process from cold and solid low-density aerogel to plasma is continuous and each step of the transition is significant for experimental results.

## References

[1] Deutsch, C. (1984). Atomic physics for beam-target interactions. *Laser and Particle Beams*, *2*(04), 449-465

[2] Deutsch, C., Maynard, G., Bimbot, R., Gardes, D., Della-Negra, S., Dumail, M., Kubica, B., Richard, A., River, M.F., Servagean, A., Fleurier, C., Sanba, A., Hoffmann, D.D.H., Weyrich, K. & Wahl, H. (1989). Ion beam-plasma interaction: A standard model approach. *Nuclear Instruments and Methods in Physics Research Section A: Accelerators, Spectrometers, Detectors and Associated Equipment, 278(1),* 38-43.

[3] Borisenko, N. G., Khalenkov, A. M., Kmetik, V., Limpouch, J., Merkuliev, Y. A., & Pimenov, V. G. (2007). Plastic aerogel targets and optical transparency of undercritical microheterogeneous plasma. *Fusion science and technology*, *51*(4), 655-664.

[4] Borisenko, N. G., Akimova, I. V., Gromov, A. I., Khalenkov, A. M., Merkuliev, Y. A., Kondrashov, V., Limpouch, J., Kuba, J., Krousky, E., Masek, K., Nazarov, V. & Pimenov, V. G. (2006). Regular 3-D networks with clusters for controlled energy transport studies in laser plasma near critical density. *Fusion science and technology*, *49*(4), 676-685.

[5] Borisenko, N. G., Nazarov, W., Musgrave, C. S. A., Merkuliev, Y. A., Orekhov, A. S., & Borisenko, L. A. (2014). Characterization of divinyl benzene aerogels with density gradient using X-ray tomography technique. *Journal of Radioanalytical and Nuclear Chemistry*, *299*(2), 961-964.

[6] Khalenkov, A. M., Borisenko, N. G., Kondrashov, V. N., Merkuliev, Y. A., Limpouch, J., & Pimenov, V. G. (2006). Experience of micro-heterogeneous target fabrication to study energy transport in plasma near critical density. *Laser and Particle Beams*, 24(02), 283-290.

[7] Akimova, I. V., Akunets, A. A., Borisenko, L. A., Gromov, A. I., Merkuliev, Y. A., & Orekhov, A. S. (2014). Metals produced as nano-snow layers for converters of laser light into X-ray for indirect targets and as intensive EUV sources. *Journal of Radioanalytical and Nuclear Chemistry, 299(2)*, 955-960.

[8] Maeder, R., Rienecker, T., Rosmej, O. N., Martsovenko, D., Borisenko, L., Malikova, A., Schachinger, M., Schönlein, A., Zaehter, S., Xu, G. & Jacoby, J. (2013). Measurements of the Heavy Ion Stopping in X-ray heated low-density nanostructured targets. *GSI Scientific Report 2012, 2013(1)*, 330.

[9] Rosmej, O. N., Klir, D., Rezak, K., Schächinger, M., Rienecker, T., Vergunova, G., Borisenko, N., Borisenko, L. & Malikova, A. (2013). Supersonic radiation

driven heat waves in foam target heated by X-rays. *GSI Scientific Report 2012, 2013(1)*, 337.

[10]     Martsovenko, D., Suslov, N., Faik, S., Basko, M., Tauschwitz, An., Borisenko, L., Malikova, A., Schadinger, M., Schönlein, A., Zaehter, S., Ge, X. & Jacoby, J. (2013). Comparison of measured time resolved hohlraum radiation temperature with data produced by RALEF II-Code. *GSI Scientific Report 2012, 2013(1)*, 338.

[11]     Rosmej, O. N., Bagnoud, V., Eisenbarth, U., Vatulin, V., Zhidkov, N., Suslov, N., Kunin, A., Pinegin, A., Schafer, D., Nisius, Th., Wilhein, Th., Rienecker, T., Wiechula, J., Jacoby, J., Zhao, Y., Vergunova, G., Borisenko, N. & Orlov, N. (2011). Heating of low-density CHO-foam layers by means of soft X-rays. *Nuclear Instruments and Methods in Physics Research Section A: Accelerators, Spectrometers, Detectors and Associated Equipment*, *653*(1), 52-57.

[12]     Jacoby, J., Hoffmann, D. H. H., Laux, W., Müller, R. W., Wahl, H., Weyrich, K., Boggasch, E., Heimrich, B., Stockl, C., Wetzler, H. & Miyamoto, S. (1995). Stopping of heavy ions in hydrogen plasma. *Physical review letters*, *74*(9), 1550.

[13]     Zwicknagel, G. (2009). Theory and simulation of heavy ion stopping in plasma. *Laser and Particle Beams*, *27*(03), 399-413.

[14]     Roth, M., Stöckl, C., Süß, W., Iwase, O., Gericke, D. O., Bock, R., ... & Seelig, W. (2000). Energy loss of heavy ions in laser-produced plasmas. *EPL (Europhysics Letters)*, *50*(1), 28.

[15]     Hu, Z. H., Song, Y. H., Mišković, Z. L., & Wang, Y. N. (2011). Energy dissipation of ion beam in two-component plasma in the presence of laser irradiation. *Laser and Particle Beams-Pulse Power and High Energy Densities*, *29*(3), 299.

[16]     Nersisyan, H. B., & Deutsch, C. (2011). Stopping of ions in a plasma irradiated by an intense laser field. *Laser and Particle Beams-Pulse Power and High Energy Densities*, *29*(4), 389.

[17]     Ogawa, M., Neuner, U., Kobayashi, H., Nakajima, Y., Nishigori, K., Takayama, K., Iwase, O., Yoshida, M., Kojima, M., Hasegawa, J., Guri, Y., Horioka, K., Nakajima, M., Miyamoto, S., Dubenkov, V. & Murakami, T. (2000). Measurement of stopping power of 240 MeV argon ions in partially ionized helium discharge plasma. *Laser and Particle Beams*,*18*(04), 647-653.